DOI: 10.1007/s41230-017-6094-2

Effects of Cu addition on microstructure and mechanical properties of as-cast Mg-6Zn magnesium alloy

Yu Zhang, *Xiao-feng Huang, Ying Ma, Ti-jun Chen, Yuan-dong Li and Yuan Hao

State Key Laboratory of Advanced Processing and Recycling of Nonferrous Metals, Lanzhou University of Technology, Lanzhou 730050, China

Abstract: The application of Mg-Zn binary alloys is restricted due to their developed dendritic microstructure and poor mechanical properties. In this study, an alloying method was used to improve the mechanical properties of Mg-Zn alloy. The Mg-6Zn magnesium alloys microalloyed with varying Cu content (0, 0.8, 1.5, 2.0 and 2.5wt.%) were fabricated by permanent mould casting, and the effects of Cu content on the microstructure and mechanical properties of as-cast Mg-6Zn alloys were studied using OM, SEM, XRD and tensile tests at room temperature. The obtained results show that the addition of Cu not only can refine the grains effectively, but also can modify the eutectic morphology and improve the mechanical properties of the alloys. The main phases of the studied alloys include α-Mg, $MgZn_2$, Mg_2Cu and CuMgZn. When the content of Cu exceeds 0.8wt.%, Mg_2Cu phase appears. Meanwhile, the eutectic morphology is modified into dendritic shape or lamellar structure, which has an adverse effect on the tensile properties. Furthermore, among the investigated alloys, the alloy containing 0.8% Cu shows an optimal ultimate tensile strength of 196 MPa, while the alloy with 1.5wt.% Cu obtains an excellent elongation of 7.22%. The experimental alloys under different Cu contents show distinguishing fracture behaviors: the fracture of the alloy with 0.8wt.% Cu reveals a mixed mode of inter-granular and quasi-cleavage, while in other investigated alloys, the fracture behaviors are dominated by cleavage fracture.

Key words: Mg-Zn magnesium alloy; Cu addition; microstructure; mechanical property; fracture mode

CLC numbers: TG146.22 **Document code:** A **Article ID:** 1672-6421(2017)04-251-07

For decades, magnesium alloys have wide applications in the aerospace, transportation and mobile electronics industries due to their advantages such as extremely low density and good damping capacity, high specific strength and stiffness, excellent machinability and good castability [1-4]. However, commercial magnesium alloys provide limited mechanical properties, which hinder their widespread applications [5]. More particularly, to the best of our knowledge, the Mg-Zn binary alloys possess coarse dendritic microstructures, extensive hot cracking tendency, critical shrinkage cavities and porosities. These drawbacks will significantly worsen the mechanical properties of the alloy [6]. The improvement of mechanical properties is a severe and urgent challenge in magnesium alloys research fields. He et al.[7] found that the mechanical properties of magnesium alloys can be significantly improved via appropriate microalloying due to grain refinement and microstructure modification in the as-cast condition. In order to improve the microstructure and mechanical properties of Mg-Zn binary alloys, many attempts have been devoted to the research and development of high-performance new Mg-Zn based alloys. For example, Mg-Zn-Zr, Mg-Zn-RE, Mg-Zn-Cu and Mg-Zn-Al-Mn alloy systems have been developed and widely applied for some industrial products. There are some minor alloying element investigations in Mg-Zn binary alloys, for instance, adding Ag, Zr, rare earth (RE) or Cu to the Mg-Zn alloy system [8]. It is noteworthy that Cu is a cost-effective element, compared with some rare earth elements such as Ce, Nd, Y and Gd [9]. Meanwhile, the Cu plays a favorable role in improving the mechanical properties of magnesium alloys. It is well recognized that the addition of Cu not only can considerably improve the castability, but also it effectively increases the eutectic temperature of the alloy so as to complete the dissolution of solute atoms at higher temperatures [10-11]. Furthermore, the dissolved Cu atoms can apparently promote the nucleation and restrain the grain growth as well as increase precipitate concentration during aging treatment. It has been

***Xiao-feng Huang**

Male, born in 1971, Ph. D, Associate professor. Research interests: magnesium alloys and semi-solid forming. To date, he has published over 70 papers..

E-mail: huangxf_lut@163.com

Received: 2016-12-16; Accepted: 2017-04-03

reported that the Mg-Zn-Cu alloys exhibit relatively high ductility and high strength owing to the grain refinement caused by Cu and Zn [12]. Zhu et al. [13] investigated the effects of Cu addition on microstructure and mechanical properties of as-cast magnesium alloy ZK60. The results indicated that the alloy modified with trace Cu of (0.5–1)wt.% exhibits the optimal mechanical properties with an excellent elongation of over 9%. Therefore, it is feasible to forecast that the reasonable addition of Cu should play a beneficial role in the grain refinement and improvement of mechanical properties for Mg-Zn binary alloys at room temperature. Although the previously mentioned studies about Cu-containing magnesium alloys have been reported widely, the effects of Cu addition on the eutectic morphology and relationship between eutectic morphology and mechanical properties of as-cast Mg-6Zn based alloys have been investigated rarely. Hence, in this study, Mg-6Zn-*x*Cu alloys (*x*=0, 0.8, 1.5, 2.0 and 2.5wt.%) microalloyed with different contents of Cu were designed and investigated systematically, so as to provide a serviceable basis for developing new low-cost Cu-containing magnesium alloys.

1 Experimental procedure

The Mg-6Zn based alloys with different Cu contents (0, 0.8, 1.5, 2.0 and 2.5%, in weight percent unless stated otherwise) were prepared from commercial high purity Mg (>99.99%), Zn ingot (>99.999%) and Cu sheet (>99.99%). All the raw alloys were preheated to 200 °C, and then the pure Mg ingot was melted in an electric resistance furnace with a mild steel crucible under protection of Ar atmosphere and a covering agent RJ-2. After the pure Mg ingot was completely melted, the Zn ingot was added into the melt. When the melt temperature was increased to approximately 720 °C, the Cu lump was added to the melt. Then the melt was held at 750 °C for 20 min for the homogenization of alloying elements. Subsequently, 2% (ratio to the whole raw metal) C_2Cl_6 was added to the melt by mechanical stirring for deslagging at 730 °C. After refining, the melt was isothermally maintained for 20 min at this temperature for the settlement of inclusions, and then, at 710 °C, was poured into the metallic mold preheated to 200 °C.

Metallographic specimens for microstructural observation were cut from the same position of each cast ingot with the dimension of 15 mm in diameter and 180 mm in length, and then mechanically polished according to standard metallographic technique, followed by etching using a 4vol.% HNO_3 solution in C_2H_5OH at room temperature. Then the specimens were observed using a MeF-3 optical microscope (OM) and field emission scanning electron microscope (SEM) with energy dispersive spectroscope (EDS). The phase constituents were identified by a D/max-2400 X-ray diffraction (XRD) using a Cu Kα radiation with a scanning velocity of 5 °/min and a scanning angle from 10 to 90°. The tensile specimens (a cross-section of 2 mm × 3 mm and a gauge length of 15 mm) were processed from the bottom of the obtained slabs utilizing a computer numerical-controlled wire-cutting machine, as shown in Fig. 1. The mechanical tests were performed on a WDW-100D universal material testing machine with a loading rate of 1 mm•s^{-1} at room temperature. The average of three tensile specimens was taken as ultimate tensile strength (UTS) and elongation to fracture (Ef) for each alloy. Tensile specimens for fracture observation were also conducted using SEM.

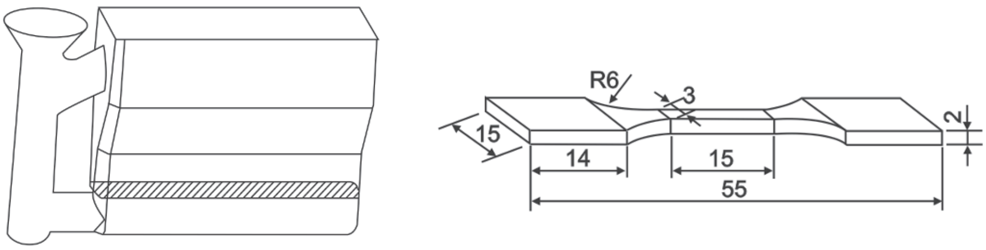

Fig. 1: Schematic for cast ingot and tensile test sample (unit: mm)

2 Results and discussion

2.1 As-cast microstructure

The XRD results of as-cast Mg-6Zn alloys containing different Cu contents are shown in Fig. 2. It can be seen that the Mg-6Zn alloy consists of α-Mg and $MgZn_2$ phases with a base-centered monoclinic structure (*a*=2.596 nm, *b*=1.428 nm, *c*=0.524 nm, *γ*=102.5°) [14]. The alloy with 0.8% Cu consists of three phases, i.e., α-Mg, $MgZn_2$ and CuMgZn phases. When the content of Cu exceeds 0.8%, the Cu-containing alloys not only include α-Mg, $MgZn_2$ and CuMgZn phases, but also contain additional diffraction peaks of Mg_2Cu phase. In addition, the number of Mg_2Cu and CuMgZu peaks increases with the increasing Cu content. The CuMgZn phase has a face-center cubic structure (*a* = 0.7169 nm, space group Fd 3m) [15].

The OM of as-cast Mg-6Zn alloys with different Cu additions is shown in Fig. 3. It can be clearly seen that all investigated alloys feature a typical non-equilibrium solidification microstructure, which is composed of matrix α-Mg, eutectic compounds and a few isolated particles distributed inside the grain. The obvious differences for the distribution of eutectic phases are observed among the alloys, namely, the distribution of eutectic phases is gradually changed from semi-continuous into completely continuous net-work morphology with increasing Cu content. In addition, the size of grains is obviously refined with an increment of Cu addition.

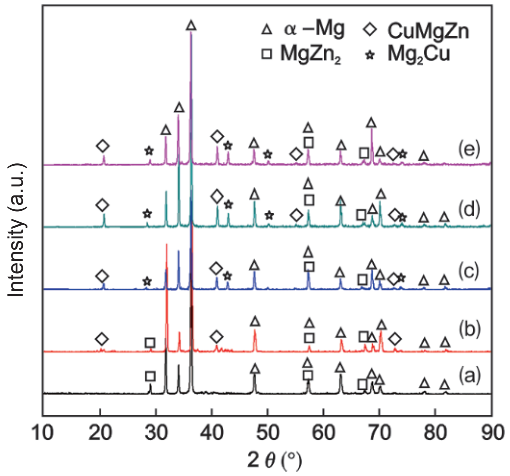

Fig. 2: XRD patterns of as-cast Mg-6Zn-*x*Cu alloys: (a) *x*=0; (b) *x*=0.8; (c) *x*=1.5; (d) *x*=2.0; (e) *x*=2.5

The microstructure of the Cu-free alloy (Fig. 3a) consists of α-Mg, secondary phases and some isolated particles within the primary dendrites. The secondary phases with continuous or semi-continuous morphology distribute along the grain boundaries. When the 0.8% Cu is added to Mg-6Zn alloy, as shown in Fig. 3(b), the amount of continuous eutectic phases obviously increases, meanwhile, the microstructure is slightly refined. With 1.5% Cu addition, it can be found from Fig. 3(c) that the microstructure contains α-Mg, continuous eutectic phases and a large amount of isolated particles inside the grains. The primary α-Mg grains show two different types of morphologies: the large dendritic grain (marked by α1) and the small granular grain (marked by α2). The secondary dendritic arm spacing (SDAS) is increased markedly, the size of grains further decreases while the eutectic phases evidently increase

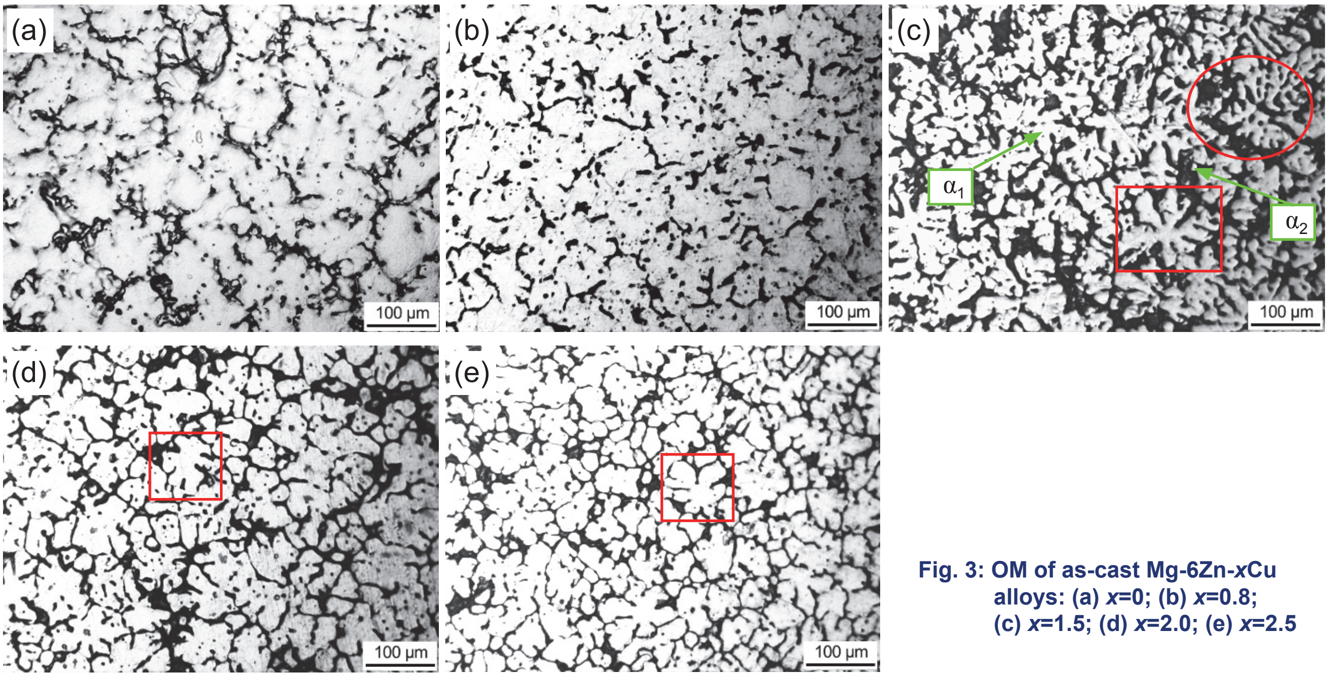

Fig. 3: OM of as-cast Mg-6Zn-*x*Cu alloys: (a) *x*=0; (b) *x*=0.8; (c) *x*=1.5; (d) *x*=2.0; (e) *x*=2.5

(comparing Fig. 3b), which is consistent with the results of the XRD analysis (Fig. 2c). According to the XRD patterns, the increased phases should be CuMgZn and Mg_2Cu. In addition, there are some eutectic phase clusters at local regions (marked by elliptical circles). When the content of Cu is continuously increased to 2.0%, the morphology of the eutectic phases is modified completely into continuous net-work form. Similarly, the primary grains with different morphologies can still be found. Furthermore, the size of grains decreases further, as compared to the alloy with 1.5% Cu. Further increasing Cu content to 2.5%, it can be clearly seen from Fig. 3(e) that the grain size of the alloy is the smallest among those of the given alloys (comparing Fig. 3a-d). The massive eutectic phases tend to distribute around grain boundaries. This is mainly due to the fact that more Cu addition can alter kinetics of precipitation reaction, resulting in the improvement of the driving force of nucleation, which increases the amount of precipitates [16]. The SDAS and the number of the independently primary α-Mg grains increase dramatically. Meanwhile, the primary α-Mg grains with different morphologies are also observed in the alloy.

It is obvious that the grain sizes of the as-cast alloys are distinctly affected by Cu content. That is to say, increasing the amount of added Cu, the grain refinement tendency of Mg-6Zn alloys intensifies (Fig. 3). This can be explained by the following reasons. On one hand, the addition of Cu can alter the solidus of the alloys, which shortens the solidification time and thus refines the microstructure [17]. On the other hand, the CuMgZn intermetallic compound possesses high melting point and good thermal stability [18]. The CuMgZn phase plays a heterogeneous nucleation substrate role in the process of solidification, which efficiently promotes the formation of crystal nucleus and thus refines grains. This stimulation effect will be improved as the added Cu content increases. In summary, the refinement efficiency of an element can be estimated by the grain refinement factor (GRF) [19]. It can be described by the following expression: $\Sigma_i m_i C_{o,i}(k_i\text{-}1)$, where m_i is the slope of the liquidus line in the binary phase diagram, $C_{o,i}$ is the initial concentration of element i and k_i is the solute distribution coefficient. According to the Mg-Cu binary phase diagram, m_{Cu} and k_{Cu} are -5.37 and 0.02, respectively. Therefore, the GRF value increases when the concentration of the element Cu is increased. Based on this viewpoint, it is easy to comprehend the decrease of grain size with the increase of Cu content from 0% to 2.5%. A large GRF not only implies large hindering effect on crystal growth, but also means that the growing crystal can generate large constitutional supercooling quickly and thus accelerate the formation of stable nuclei [20].

As can be seen from Fig. 3, the SDAS firstly decreases as the Cu content increases from 0 to 0.8%, then increases when the Cu content exceeds 0.8%. The evolution tendency is considered to be related to the following reasons. The SDAS can be evaluated by the following equations [21]:

$$\lambda_2=5.5(Mt_f)^{\frac{1}{3}} \tag{1}$$

$$M=\frac{\Gamma D\ln\left(\frac{C_l^m}{C_0}\right)}{m(1\text{-}k)(c_0\text{-}c_l^m)} \tag{2}$$

where k can be calculated as: $k=\left(\frac{C_s}{C_l}\right)$ (3)

where λ_2 is the value of SDAS, μm; t_f is the local solidification time, s; Γ is the Gibbs Thomson; D is the diffusion coefficient in liquid, $m^2{\cdot}s^{-1}$; m is the liquid slope, K/wt.%; M is the volume coarsening rate of the dendritic arm, $m^3{\cdot}s^{-1}$; C_0 is the initial alloy concentration, wt.%; $C_l^m=C_e$, the eutectic composition, wt.%; k is the distribution coefficient; C_s and C_l are the equilibrium solubility. As is well known, the as-cast grain sizes are closely related to the degree of heterogeneous nucleation and the constitutional undercooling [22]. When 0.8% Cu is added to the melt, Cu atoms will be squeezed out of the liquid ahead of the growing interface for a relatively rapid cooling rate during solidification process. As a result, it increases the solid-liquid interfacial energy, prevents the diffusion of Zn atoms, and then increases the value of C_l. According to eq. (2) and (3), the increase of C_l results in the decrease of k, and then the reduction of k leads to the decrease of M. Consequently, according to eq. (1), when 0.8% Cu is added to the alloy, λ_2 decreases distinctly, as compared to the alloy without Cu. On the contrary, when the addition of Cu is more than 0.8%, Mg_2Cu phase appears; meanwhile, the number of CuMgZn and Mg_2Cu phases tends to increase (Fig. 2c–2e), with the result that massive Cu atoms are inevitably expended due to the generation of the increased Cu-containing intermetallics during the solidification process. After these phases are formed, the grain growth will continue to proceed, while the amount of new nuclei tends to decrease because of the decrease of constitutional undercooling. Therefore, excessive Cu (>0.8%) addition leads to the increase of the SDAS.

The high-magnification SEM micrographs and the corresponding EDS analysis of the as-cast alloys are given in Fig. 4 and Table 1, respectively. As shown in Fig. 4, the eutectic morphology of the investigated alloys is evidently affected by Cu content. In the Cu-free alloy, the eutectic compound shows smooth island morphology (Fig. 4a). The bright precipitate (marked A, D, H, K and O) of the alloy is rich in Zn. Combined with the XRD results, the bright compound is confirmed to be $MgZn_2$ phase. The gray precipitate (marked B) in the Cu-free alloy mainly contains Mg; it is identified as α-Mg and $MgZn_2$ phase. The eutectic morphology of the alloy with 0.8% Cu presents flower pattern (Fig. 4b). Based on the results of the XRD, EDS and Table 1, the black area (marked C, F, I and M) is regarded as α-Mg phase, and the gray area (marked E) is identified as CuMgZn phase. With the addition of 1.5% Cu, the eutectic phases change into perfect penniform shape (Fig. 4c). As seen in Table 1, the gray one (marked G) includes Mg, Zn and Cu, and is rich in Cu (comparing points F and H), combining with the XRD results, it is regarded as Mg_2Cu and CuMgZn phase. After 2% Cu is added, the secondary phases present lamellar or dendtitic morphology (Fig. 4d), but the gray precipitates (marked J and L) have similar constituents as that of the alloy with 1.5% Cu, which are also Mg_2Cu and CuMgZn phases. When the Cu content is up to 2.5%, the whole eutectic morphology of the alloy is clearly modified; the gray intermetallics display coarsely lamellar structure (Fig. 4e). The constituent of the gray precipitate (marked N) is inferred as Mg_2Cu and CuMgZn phase according to the XRD. According to the formation mechanism of the lamellar structure reported by Du et al [23], it is reasonable to assume that the creation of lamellar structure of the alloy with more Cu (⩾ 2.0%) is due to the addition of Cu causing intensive constitutional undercooling ahead of the solid/liquid interface in the liquid layer, promoting the primary α-Mg phase solidification and the increase of Cu and Zn concentration in the liquid. As a result, the composition ahead of the solid/liquid interface attains the eutectic composition and matches within a zone of the coupled eutectic growth. Therefore, the addition of more Cu promotes to the formation of a lamellar morphology of the intermetallics.

2.2 Mechanical properties

Mechanical properties have an important relationship with the amount and distribution of the intermetallics [24]. Trace addition of Cu to the Mg-6Zn alloys causes the modification of the intermetallics morphology, which will accordingly affect the mechanical properties. Figure 5 shows the variations of the room temperature tensile properties of Mg-6Zn alloys with different Cu contents, including the ultimate tensile strength (UTS) and elongation to fracture (Ef). As shown in Fig. 5, the addition of Cu has a positive effect on the tensile properties of the investigated alloys. The considerable improvement of the tensile properties is observed, as compared to the alloy without Cu. It is found that the UTS and Ef firstly increase as the Cu content increases, and then decrease. When the 0.8% Cu is added to Mg-6Zn alloy, the UTS increases sharply to the maximum value of 196 MPa, but the Ef does not reach the peak value. Contrarily, when the content of Cu is increased to 1.5%, a peak value 7.22% of Ef is obtained. Compared with the Cu-free alloy, the peak values of UTS and Ef are enhanced by 16 MPa and 24.5%, respectively. It is well known that the fine grains are commonly beneficial to the tensile properties

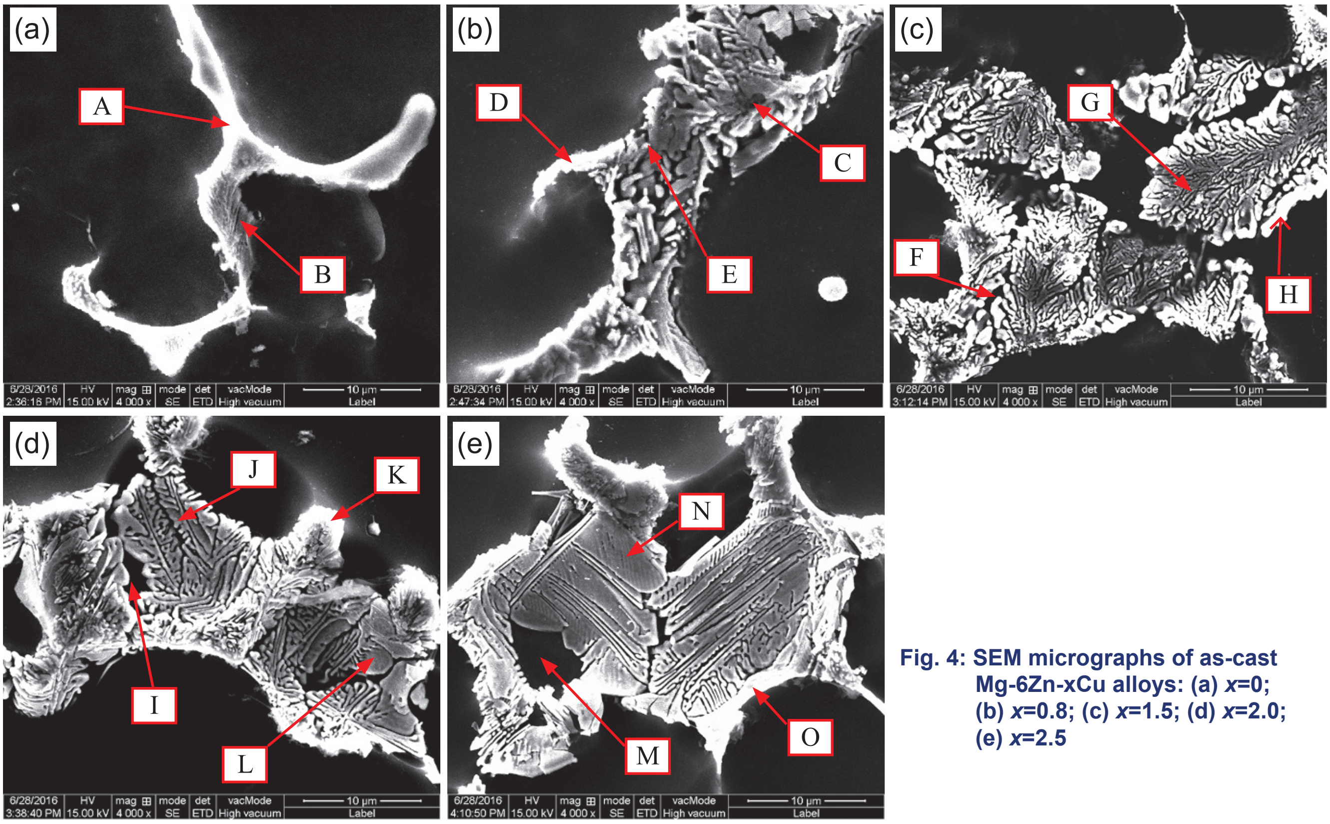

Fig. 4: SEM micrographs of as-cast Mg-6Zn-xCu alloys: (a) *x*=0; (b) *x*=0.8; (c) *x*=1.5; (d) *x*=2.0; (e) *x*=2.5

Table 1: Chemical compositions of as-cast alloys (at.%)

Location (point)	Mg	Zn	Cu
Fig. 4(a), A	65.20	34.80	0.00
Fig. 4(a), B	81.60	18.40	0.00
Fig. 4(b), C	97.50	1.70	0.80
Fig. 4(b), D	64.40	34.10	1.50
Fig. 4(b), E	78.60	13.10	8.30
Fig. 4(c), F	97.48	1.65	0.87
Fig. 4(c), G	75.40	14.10	10.50
Fig. 4(c), H	65.70	33.80	0.50
Fig. 4(d), I	97.30	2.70	0.00
Fig. 4(d), J	57.80	28.20	14.00
Fig. 4(d), K	68.17	31.10	0.73
Fig. 4(d), L	68.10	20.20	11.70
Fig. 4(e), M	98.40	1.60	0.00
Fig. 4(e), N	51.70	28.60	19.70
Fig. 4(e), O	64.08	35.10	0.82

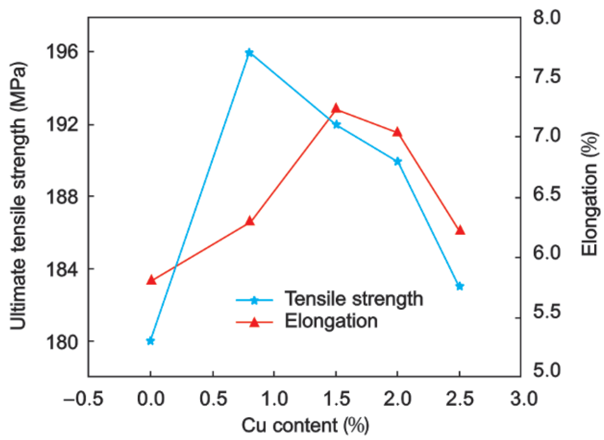

Fig. 5: Room-temperature tensile properties of as-cast Mg-6Zn-xCu alloys

of engineering alloys [25]. In addition, as far as we know, the microstructural inhomogeneity has been an issue in many binary Mg-Zn alloys [26]. The increase of tensile properties is due to that the Cu addition can offer a valuable solution to the microstructural inhomogeneity for the investigated alloys and effectively decrease the grain sizes of the alloys. When the content of Cu is over 0.8% and 1.5%, the UTS and Ef have a trend to decline. The UTS and Ef decrease from peak values of 196 MPa (0.8% Cu) and 7.22% (1.5% Cu) to 183 MPa and 6.21%, respectively, when Cu addition reaches 2.5%. The degradation of tensile properties is mainly ascribed to the following two reasons: (1) A higher addition of Cu (≥1.5%) causes the formation of the Mg_2Cu compounds (Fig. 2) and increase of eutectic phase amounts. In addition, the eutectic morphology is modified into dendritic shape or lamellar structure, which acts as crack initiation sites during tensile testing, thus deteriorating the tensile properties. This is mainly due to the fact that high stress concentration will be produced in the vicinity of a large number of second phases [27], which might cause the crack initiation and reduce the mechanical properties. (2) Furthermore, with the increment of Cu content, the primary α-Mg grains are surrounded by the continuous agglomerates, which probably play an adverse role in increasing the tensile properties [28]. In a word, the dendritic shape or lamellar structure and continuous agglomerates are responsible for the decrease in the tensile properties. By comparison of the mechanical properties of the investigated alloys, it can be concluded that a proper content of Cu (0.8%–1.5%) can dramatically enhance the tensile properties of the as-cast Mg-6Zn base alloys at room temperature.

2.3 Fracture analysis

The cleavage fracture, quasi-cleavage fracture and inter-granular fracture are the main fracture modes of magnesium alloys [29]. Figure 6 shows the SEM images of tensile fracture surfaces of the studied alloys with different Cu contents. As shown in Fig. 6(a), in the alloy without Cu, several porosities are found; meanwhile, some tear ridges and cleavage planes can also be observed. The generation of the porosities is attributed to molten metal being scarce in these areas. This is because the relatively rapid cooling rate leads to these porosities are not padded by the corresponding molten metal in the subsequent solidification process. The fracture surfaces of the alloy with 0.8% Cu are characterized by many small cleavage facets, tear ridges, cleavage steps and some subtle dimples, indicating that the tensile fracture surfaces have mixed characteristics of inter-granular and quasi-cleavage fractures. In Fig. 6(c), a few cleavage planes and a small number of tearing ridges present and some porosities are also found in the local areas of tensile fracture surfaces for the alloy with 1.5% Cu. These porosities are possibly associated with oxide inclusions. With 2% Cu addition, as shown in Fig. 6(d), the fracture surfaces mainly consist of a few ambiguous cleavage planes, tearing ridges and visible cracks. The cracks are possibly related to the dendritic morphology and lamellar structure of the eutectic phase of the alloy. Yang et al [30] pointed out that the initiation of micro-cracks can be greatly influenced by the presence and nature of the secondary phases. Therefore, it can be speculated that the Cu-bearing phase probably plays a potential role in the formation of the nucleation sites of microcracks. When the content of Cu is up to 2.5%, as shown in Fig. 6(e), a small number of tearing ridges and massive cracks are observed. According to the fracture characteristics, the fracture behavior of the alloy is inter-granular pattern.

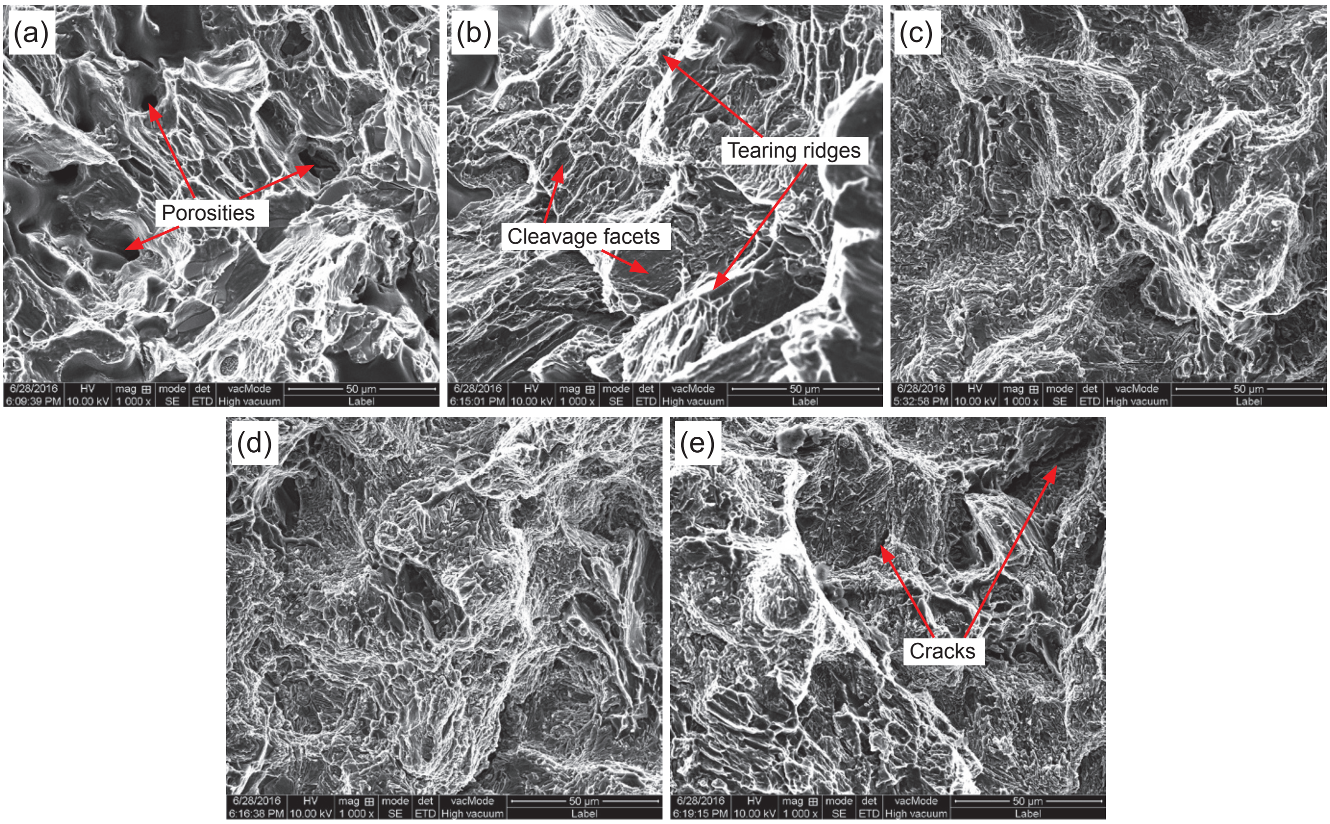

Fig. 6: SEM micrographs of tensile fracture surface of as-cast Mg-6Zn-*x*Cu alloys: (a) *x*=0; (b) *x*=0.8; (c) *x*=1.5; (d) *x*=2.0; (e) *x*=2.5

3 Conclusions

(1) The addition of Cu has significant effects on the phase constituent and microstructure of as-cast Mg-6Zn based alloys. Varied phase constituents, including $MgZn_2$, Mg_2Cu and CuMgZn, are obtained by adjusting the content of Cu. The amount of eutectic compounds increases while the grain sizes gradually decrease with the incremental addition of Cu.

(2) Cu can modify the eutectic morphology from a smooth island (the base alloy) to flower pattern, perfectly penniform shape, lamellar or dendritic shape (with 0.8%–2.0% Cu), and then to coarsely lamellar structure (with 2.5% Cu). When the addition of Cu exceeds 0.8%, the SDAS has a tendency to increase.

(3) The small amount of Cu (0.8%) addition results in considerable increases of the UTS, giving a maximum UTS value of 196 MPa, while a peak value of Ef (7.22%) is obtained when the content of Cu is 1.5%. However, an excessive Cu addition (⩾1.5% Cu) will substantially deteriorate the tensile properties of the alloys.

(4) The experimental alloys under different Cu contents show different fracture behaviors: in Mg-6Zn-(0–2.5)Cu alloy, the fracture behavior of the alloys reveals cleavage fracture while the alloy with 0.8% Cu exhibits a mixed fracture of inter-granular and quasi-cleavage fracture with ductile rupture characterized by dimples, tear ridges and cleavage steps.

References

[1] Zhu H M, Luo C P, Liu J W, et al. Growth twinning behavior of cast Mg-Zn-Cu-Zr alloys. Transactions of Nonferrous Metals Society of China, 2014, 24(2): 316–320.
[2] Wang W, Xu C X, Zhang J S, et al. Effects of Ce addition on microstructure, mechanical properties and corrosion resistance of as-cast AZ80 magnesium alloy. China Foundry, 2014, 11(3): 157–162.
[3] Wang J F, Gao S, Song P F, et al. Effects of phase composition on the mechanical properties and damping capacities of as-extruded Mg-Zn-Y-Zr alloys. Journal of Alloys and Compounds, 2011, 509(34): 8567–8572.
[4] Ming Y, Zheng Z Q. Effects of Zn on the microstructures and mechanical properties of Mg-3Sm-0.5Gd-*x*Zn-0.5Zr (*x*=0, 0.3 and 0.6) alloy. Journal of Alloys and Compounds, 2014, 590: 355–361.
[5] Luo A A, Mishra R K, Powell B R, et al. Magnesium alloy development for automotive applications. Materials Science Forum, 2012, 706–709: 69–82.
[6] Chen Zhenhua. Magnesium Alloys. Beijing: Chemical Industry Press, 2004; pp. 312–313.
[7] He S M, Zeng X Q, Peng L M, et al. Microstructure and strengthening mechanism of high strength Mg-10Gd-2Y-0.5Zr alloy. Journal of Alloys and Compounds, 2007, 427(1–2): 316–323.
[8] Wei S H, Zhu T P, Michael H, et al. Effects of lead addition on the microstructure and mechanical properties of as-cast Mg-4Zn alloys. Materials Science and Engineering A, 2012, 550: 199–205.
[9] Yu H, Yu H S, Kin Y M, et al. Hot deformation behavior and processing maps of Mg-Zn-Cu-Zr magnesium alloy. Transactions of Nonferrous Metals Society of China, 2013, 23(3): 756–764.
[10] LI Aiwen, LIU Jiangwen, WU Cuilan, et al. Age-hardening behavior and precipitates of as-cast Mg-3Zn-1.5Cu-0.6Zr Mg alloy. The Chinese Journal of Nonferrous Metals, 2010, 20(6): 1053–1059.
[11] Buha J. Mechanical properties of naturally aged Mg-Zn-Cu-Mn alloy. Materials Science and Engineering A, 2008, 489(1–2): 127–137.
[12] Golmakaniyoon S, Mahmudi R. Microstructure and creep behavior of the rare-earth doped Mg-6Zn-3Cu cast alloy. Materials Science and Engineering A, 2011, 528(3): 1668–1677.
[13] Zhu H M, Luo C P, Liu J W, et al. Effects of Cu addition on microstructure and mechanical properties of as-cast magnesium alloy ZK60. Transactions of Nonferrous Metals Society of China, 2014, 24(3): 605–610.
[14] Zhang D F, Shi G L, Zhao X B, et al. Microstructure evolution and mechanical properties of Mg-*x*%Zn-1%Mn (*x*=4, 5, 6, 7, 8, 9) wrought magnesium alloys. Transactions of Nonferrous Metals Society of China, 2011, 21(1): 15–25.
[15] Chen X H, Liu L Z, Pan F S, et al. Microstructure, electromagnetic shielding effectiveness and mechanical properties of Mg-Zn-Cu-Zr alloys. Materials Science and Engineering B, 2015, 197: 67–74.
[16] Liao Y G, Han X Q, Zeng M X, et al. Influence of Cu on microstructure and tensile properties of 7XXX series aluminum alloy. Materials and Design, 2015(66): 581–586.
[17] Buha J, Ohkubo T. Natural aging in Mg-Zn(-Cu) alloys. Metallurgical and Materials Transactions A, 2008, 39(9): 2259–2273.
[18] Zhu H M, Sha G, Liu J W, et al. Microstructure and mechanical properties of Mg-6Zn-xCu-0.6Zr (wt.%) alloys. Journal of Alloys and Compounds, 2011, 509(8): 3526–3531.
[19] Lee Y C, Dahle A K, StJohn D H. The role of solute in grain refinement of magnesium. Metallurgical and Materials Transactions A, 2000, 31(11): 2895–2906.
[20] Dahle A K, Lee Y C, Nave M D. Development of the as-cast microstructure in magnesium-aluminium alloys. Journal of Light Metals, 2001(1): 61–72.
[21] Qiu H X, Yan H, Hu Z. Effect of samarium (Sm) addition on the microstructures and mechanical properties of Al-7Si-0.7Mg alloys. Journal of Alloys and Compounds, 2013, 567(15): 77–81.
[22] Zhang Y, Huang X F, Ma Z D, et al. The influences of Al content on the microstructure and mechanical properties of as-cast Mg-6Zn magnesium alloys. Materials Science & Engineering A, 2017, 686: 93–101.
[23] Du Y Z, Qiao X G, Zheng M Y, et al. Effect of microalloying with Ca on the microstructure and mechanical properties of Mg-6 mass%Zn alloys. Materials and Design, 2016, 98: 285–293.
[24] Chen T J, Zhang D H, Wang W, et al. Effects of Y content on microstructures and mechanical properties of as-cast Mg-Zn-Nd alloys. China Foundry, 2015,12(5): 339–348.
[25] Balasubramani N. Optimization of heat treatment parameters in ZA84 magnesium alloy. Journal of Alloys and Compounds, 2008, 457(1–2): 118–123.
[26] Unsworth W. New magnesium alloys for automobile applications. Light Metal Age, 1987, 45(7–8): 10–13.
[27] Sung H P, Jung J G, Yoon J, et al. Influence of Sn addition on the microstructure and mechanical properties of extruded Mg-8Al-2Zn alloy. Materials Science and Engineering A, 2015, 626: 128–135.
[28] Bai Y, Fang C F, Hao H, et al. Effects of yttrium on microstructure and mechanical properties of Mg-Zn-Cu-Zr alloys. Transactions of Nonferrous Metals Society of China, 2010, 20(s2): 357–360.
[29] Acer E, Çadırl E, Erol H, et al. Effect of heat treatment on the microstructures and mechanical properties of Al-5.5Zn-2.5Mg alloy. Materials Science & Engineering A, 2016, 662: 144–156
[30] Yang M B, Wu D Y, Hou M D, et al. As-cast microstructures and mechanical properties of Mg-4Zn-*x*Y-1Ca (*x*=1.0, 1.5, 2.0, 3.0) magnesium alloys. Transactions of Nonferrous Metals Society of China, 2015, 25(3): 721–731.

This work was financially supported by the National Nature Science Foundations of China (51464032) and the National Basic Research Program of China (grant No. 2010CB635106).